JGR Biogeosciences

RESEARCH ARTICLE
10.1029/2019JG005186

Special Section:
Water-Energy-Carbon Fluxes Over Terrestrial Water Surfaces

Large Spatial and Temporal Variability of Carbon Dioxide and Methane in a Eutrophic Lake

Luke C. Loken[1], John T. Crawford[2], Paul J. Schramm[1], Philipp Stadler[3,4], Ankur R. Desai[5], and Emily H. Stanley[1]

[1]Center for Limnology, University of Wisconsin-Madison, Madison, WI, USA, [2]Institute of Arctic and Alpine Research, University of Colorado Boulder, Boulder, CO, USA, [3]Centre for Water Resource Systems, TU Wien, Vienna, Austria, [4]Institute for Water Quality-Resources and Waste Management, TU Wien, Vienna, Austria, [5]Atmospheric and Oceanic Sciences, University of Wisconsin-Madison, Madison, WI, USA

Key Points:
- Concentrations of carbon dioxide and methane in Lake Mendota varied through time and across the lake surface
- Efflux estimates at the lake center overestimated lakewide carbon dioxide emissions and underestimated methane emissions to the atmosphere
- Upscaling concentrations, fluxes, and gas transfer velocities from point samples to whole lakes requires consideration of spatial variability

Supporting Information:
- Supporting Information S1

Correspondence to:
L. C. Loken,
lloken@wisc.edu

Citation:
Loken, L. C., Crawford, J. T., Schramm, P. J., Stadler, P., Desai, A. R., & Stanley, E. H. (2019). Large spatial and temporal variability of carbon dioxide and methane in a eutrophic lake. *Journal of Geophysical Research: Biogeosciences*, *124*, 2248–2266. https://doi.org/10.1029/2019JG005186

Received 4 APR 2019
Accepted 18 JUN 2019
Accepted article online 2 JUL 2019
Published online 22 JUL 2019

Abstract Lakes are conduits of greenhouse gases to the atmosphere; however, most efflux estimates for individual lakes are based on extrapolations from a limited number of locations. Within-lake variability in carbon dioxide (CO_2) and methane (CH_4) arises from differences in water sources, mixing, atmospheric exchange, and biogeochemical transformations, all of which vary across multiple temporal and spatial scales. We asked, how variable are CO_2 and CH_4 across the surface of a single lake, how do spatial patterns change seasonally, and how well does the typical sampling location represent the entire lake surface? During the 2016 ice-free period, we mapped surface water concentrations of CO_2 and CH_4 approximately weekly in Lake Mendota (USA) and modeled diffusive gas exchange. During stratification, CO_2 was generally lower than atmospheric saturation (mean 19.81 μM) and relatively homogenous (mean coefficient of variation 0.12), whereas CH_4 was routinely extremely supersaturated (mean 0.29 μM) with greater spatial heterogeneity (mean coefficient of variation 0.65). During fall mixis, concentrations of both gases increased and became more spatially variable, but their spatial arrangements differed. In this system, samples collected from the lake center reasonably well represented the spatially weighted mean CO_2 concentration but overestimated annual CO_2 efflux by 21%. For CH_4, the lake center underestimated annual diffusive efflux by only 8.6% but poorly represented lakewide concentrations and fluxes on any given day. Upscaling from a single site to the whole lake requires consideration of spatial variation to assess lakewide carbon dynamics due to heterogeneity in within-lake processing, transport to the lake surface, and exchange with the atmosphere.

Plain language summary Numerous physical, chemical, and biological properties vary across the surface of individual lakes. However, researchers frequently use the lake center to represent the entire lake and ignore spatial heterogeneity. Using a boat-mounted sampling system, we mapped carbon dioxide and methane across the surface of Lake Mendota 26 times spanning the entire ice-free season. We described the progression of each gas's spatial pattern and evaluated the consequences of using only the lake center to calculate emissions to the atmosphere. The lake surface alternated between periods of relative uniformity to periods or remarkable spatial heterogeneity, and the spatial patterns of the two gases did not always align. At the annual scale, samples at the lake center overestimated lakewide carbon dioxide efflux and underestimated methane efflux. These results have consequences for our understanding of lake carbon cycling and the contribution of lakes to atmospheric greenhouse gas budgets.

1. Introduction

Lakes are important regulators of global carbon cycling and conduits of greenhouse gases to the atmosphere (Cole et al., 2007; Tranvik et al., 2009). Collectively, lakes emit globally consequential amounts of carbon dioxide (CO_2) and methane (CH_4) to the atmosphere (DelSontro, Beaulieu, & Downing, 2018; Myhre et al., 2013); however, most lake-specific emission estimates rely on extrapolations from a limited number of locations (Bastviken et al., 2004; Rasilo et al., 2015; Sobek et al., 2005). These estimates are useful in assessing seasonal dynamics and comparing among lakes, but they may not accurately represent the entire lake surface because they do not sufficiently account for within-lake spatial variation. The distribution of greenhouse gases and other chemical and biological constituents is unevenly distributed across the surface waters of individual lakes (Crawford et al., 2015; Rinke et al., 2009; Van de Bogert et al., 2012), and this spatial

heterogeneity is likely to lead to inaccurate and/or highly uncertain estimates of effluxes for the lake as a whole (Beaulieu et al., 2016; Natchimuthu et al., 2016; Schilder et al., 2013; Wik et al., 2016).

Spatial variability in CO_2 and CH_4 within individual lakes arises from differences in water sources, physical mixing, and local transformations. River and groundwater inputs to lakes are often supersaturated in CO_2 (McDonald et al., 2013; Raymond et al., 2013) and CH_4 (Paytan et al., 2015; Stanley et al., 2016) and likely differ in concentration from the receiving lake, requiring physical mixing to achieve homogenous lake conditions. The existence of river plumes that create contrasts in nearshore water chemistry (Cooney et al., 2018; Mackay, Jones, Folkard, & Thackeray, 2011; Zhang et al., 2016) and biotic activity (Makarewicz et al., 2012; Wynne & Stumpf, 2015) are clear reminders that incoming waters do not instantaneously mix across a lake.

Additionally, within-lake spatial variability results from differences in biogeochemical and physical processes and rates among lake habitats. Aquatic plant growth in littoral areas can affect local metabolic rates (Goodwin et al., 2008; Lauster et al., 2006) and retard water exchange (Nepf & Vivoni, 2000), which can result in lower CO_2 nearshore during times of high productivity (e.g., Peixoto et al., 2016; Schilder et al., 2013). Similarly, heterogeneity within pelagic zones may reflect temporal and spatial variability in phytoplankton abundance. Algae and cyanobacteria often develop in patches across the surface of lakes (Butitta et al., 2017; George & Heaney, 1978; Wynne & Stumpf, 2015), potentially lowering CO_2 concentrations and emissions during bloom events in locations with higher phytoplankton densities (Balmer & Downing, 2011; Ouyang et al., 2017). For CH_4, littoral zones often have elevated concentrations compared to offshore waters (Hofmann, 2013; Natchimuthu et al., 2016; Schilder et al., 2013). While CH_4 can be produced in oxygenated surface waters (Bogard et al., 2014; Tang et al., 2016), most CH_4 generation is attributed to anoxic environments, especially lake sediments (Hofmann, 2013; Peeters et al., 2019). Compared to the profundal zone, littoral sediments are not isolated through stratification, have elevated temperatures, and are more easily disrupted by surface waves, all of which aid in CH_4 delivery to nearshore surface waters (Bastviken et al., 2008; Hofmann et al., 2010; Murase et al., 2005). The fact that differences in water chemistry occur within individual lakes (Crawford et al., 2015; Hofmann, 2013; Schilder et al., 2013) indicates that in some lakes physical mixing does not completely overwhelm local processing and sourcing. Although others have demonstrated the importance of spatial heterogeneity for evaluating CO_2 and CH_4 dynamics within lakes (e.g., Natchimuthu et al., 2017; Wik et al., 2016), most studies lack high-resolution coverage in both space and time. The mechanisms responsible for creating or eroding spatial patterns respond to changes in environmental drivers (e.g., temperature, wind, river discharge, and stratification) at multiple temporal scales (Butitta et al., 2017; Cooney et al., 2018; Natchimuthu et al., 2016). Thus, assessing spatial heterogeneity in lakes requires a temporally dynamic framework. The balance between local transformations and water movements will ultimately determine the spatial pattern of water chemistry in aquatic ecosystems (Pinel-Alloul, 1995).

While spatial variation in CO_2 and CH_4 concentrations can drive differences in fluxes to the atmosphere, we also need to consider the rate at which these gases move across the air-water interface. Diffusive flux is often modeled based on the concentration gradient across the air-water interface and the gas transfer velocity (k), which is typically modeled using wind speed, lake size, and/or water temperature (Cole & Caraco, 1998; Read et al., 2012; Vachon & Prairie, 2013). These models recognize the variability in k through time and among lakes, yet to the best of our knowledge, only one (Vachon & Prairie, 2013) acknowledges the spatial heterogeneity of k within individual lakes attributable to variability in wind-driven surface turbulence. If lake regions consistently have large k values and elevated gas concentrations, the resulting flux would be substantial. Therefore, we should consider the spatial arrangement of gas concentration and k together to fully assess the lakewide emission rates.

In this paper, we ask (1) how variable are CO_2 and CH_4 surface water concentrations and fluxes within a single lake, 2) how do the spatial patterns of CO_2 and CH_4 change temporally, and (3) how well do single point samples at the lake center represent the entire lake surface. The physical and biogeochemical spatial heterogeneity of lakes leads to questions regarding the validity of whole-lake estimates based on single-point measurements. We predicted that CO_2 emission estimates based on conditions at the lake center would consistently overestimate lakewide CO_2 efflux due to the influence of primary production in littoral and river-influenced environments. In contrast, we suspected that pelagic-based CH_4 emission rates substantially underestimated lakewide diffusive efflux, as shallow environments produce and deliver more CH_4 to the

lake surface. However, the processes driving the formation and/or breakdown of spatial heterogeneity may be temporally dynamic, potentially causing the spatial patterns to continually evolve. Comprehensive assessments of spatial heterogeneity in lakes are rare in the literature, which limits our understanding of lake carbon cycling and may have a significant impact on our perception of the contribution of lakes to global greenhouse gas inventories.

2. Methods

2.1. Site Description

Lake Mendota is a 39.9-km^2 eutrophic lake and is regularly monitored by the North Temperature Lakes-Long Term Ecological Research (NTL-LTER; lter.limnology.wisc.edu) program. The lake is located in a low topographic relief region of Southern Wisconsin, USA (43.1°N, 89.4°W). The lake has a maximum depth of 25.3 m (mean 12.7 m) and a mean water residence time of 4.5 years. Lake Mendota is dimictic with thermal stratification typically occurring between May and October and ice cover from late December to March (mean ice duration from 2006 to 2016 was 88 days). Approximately 70% of the lake's water budget comes from the Yahara River and Sixmile Creek (Brock, 1985). Both rivers drain predominately agricultural watersheds (Homer et al., 2015; Lathrop & Carpenter, 2013) and flow into the lake's northern bay (Figure 1). Blooms of green algae and cyanobacteria commonly occur during the warmer periods because of elevated nutrient levels (mean surface total phosphorus concentration during 2006–2016 was 0.08 mg P/L). Due to high productivity, the hypolimnion usually becomes anoxic by mid-June. NTL-LTER maintains a buoy on Lake Mendota (43.100°N, 89.405°W) moored at the lake's deepest point (Figure 1). The buoy was equipped with a thermistor string (RBR concerto) and anemometer (R. M. Young Marine Wind Monitor) that measured water temperature (at 23 depths) and wind (speed and direction), respectively.

2.2. Sampling Design

To investigate the spatial heterogeneity of Lake Mendota, we used the FLAMe sampling platform (Crawford et al., 2015). The FLAMe is a spatially explicit sampling system that integrates automated limnological sensors into a mobile platform. Briefly, surface water (~0.2-m depth) was pumped onboard a moving boat to a series of water sensors including a YSI-EXO2 (outfitted with temperature, specific conductivity, pH, dissolved oxygen, algal fluorescence, turbidity, and fluorescent dissolved organic matter sensors for this study) and a Satlantic SUNA V2 optical nitrate sensor that we programed to capture data at 1 and ~0.1 Hz, respectively. Water was then delivered to a shower-type equilibrator (Crawford et al., 2015) where dissolved gases equilibrated in an enclosed headspace. We then were able to continually measure gas-phase CO_2 and CH_4 at 1 Hz using a Los Gatos Research ultraportable greenhouse gas analyzer (UGGA). Equilibrated gas partial pressures were converted to dissolved concentrations (μM) using atmospheric pressure and water temperature according to Henry's law and temperature-dependence models supplied in Plummer and Busenberg (1982) and Wilhelm et al. (1977) for CO_2 and CH_4, respectively (see the supporting information for more details).

We georeferenced the YSI-EXO2, SUNA, and UGGA outputs with a Garmin Echomap 50s GPS (WAAS enabled) and corrected them for hydraulic lags and sensor response rates using methods outlined in Crawford et al. (2015) and Fofonoff et al. (1974). Because the boat constantly moves, sensor measurements never reach equilibrium, and point measurements reflect conditions over a preceding interval of time. We determined first-order response characteristics of each sensor (Table S2) and applied an ordinary differential equation to spatially correct measurements. This procedure resolved water-based measurements (e.g., pH and algal fluorescence) to within 10 s and resolved gas measurements (i.e., CO_2 and CH_4) to within 30 s. The additional time needed for the gases results from them being extracted from the water (Webb et al., 2016), pumped to the UGGA, and measured in the gas phase. Thus, each corrected measurement integrates water conditions over the previous 10 to 30 s. Combining this temporal resolution with a boat traveling upward of 30 km/hr, we derived a spatial resolution of up to 250 m. The spatially corrected values should not be considered as point measurements, but rather a representation of the water surface at a spatial resolution of ~250 m.

We surveyed Lake Mendota on 26 days (every 1 to 2 weeks) over the 2016 open water season (29 March to 2 December). On each sampling day, we continually measured surface water conditions while motorboating

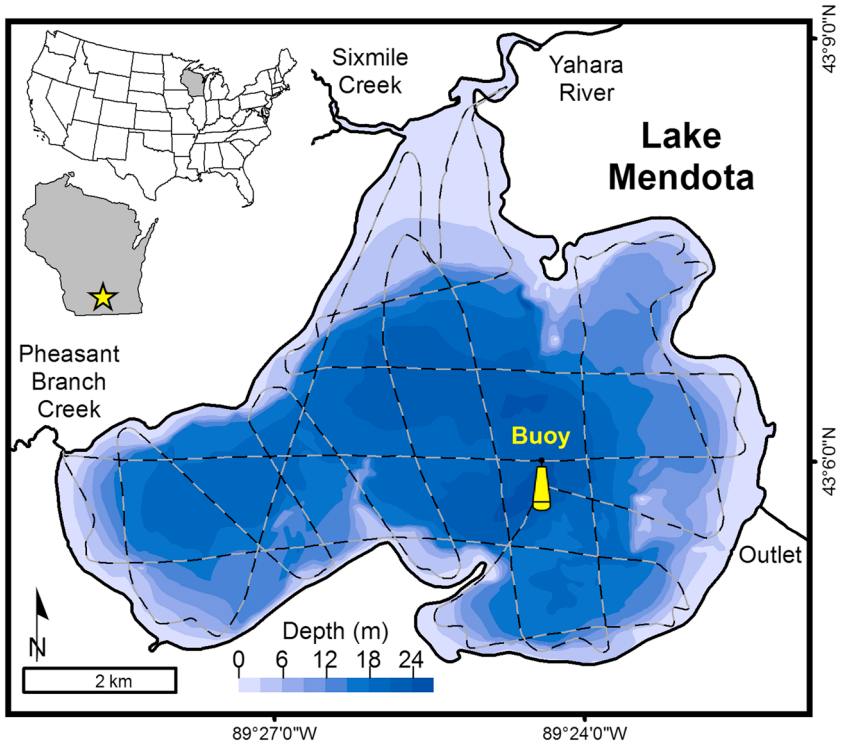

Figure 1. Lake Mendota bathymetry, major rivers, and sampling track (line). Each sampling event started and ended at the Long Term Ecological Research sampling buoy (yellow) that is located above the lake's deepest point.

(5-m Boston Whaler with a gas-powered outboard motor) along an established sample route (Figure 1). For most of the survey, we traveled at 25 to 30 km/hr, but we reduced our speed to ~8 km/hr in several shallow nearshore areas. Our route began and ended at the buoy, and we alternated track direction among sample dates. Our sample path included both north-south and east-west transects across the entire lake surface and several shorter segments nearshore. In this fashion, we obtained widely spaced transects in the middle of the lake and a greater density of data across littoral-pelagic transitions, as we expected more variation nearshore due to the existence of river inlets and heterogeneous littoral habitats. Each sampling survey occurred in the morning (08:00–12:00) and lasted ~3 hr. To simulate our "buoy" sample and to assess temporal dynamics during our spatial survey, we stopped the boat at the buoy preceding and succeeding each spatial survey, allowed the FLAMe system to stabilize for at least 5 min, and averaged 1 min of sensor data. We also measured atmospheric CO_2 and CH_4 at the buoy using the UGGA, which we used to calculate equilibrium concentrations and to model diffusive flux (see below).

2.3. Modeling

From each spatial survey, we obtained ~10,000 point observations, which were used to model CO_2 and CH_4 (and other variables) across the contiguous lake surface. Spatial modeling and analyses were done using the programming language R (R Core Team, 2018). Concentrations were estimated at an evenly spaced grid (i.e., pixels) using an inverse distance weighting model:

$$Z_j = \sum_i \frac{Z_i}{{d_{ij}}^2} \div \sum_i \frac{1}{{d_{ij}}^2}, \quad (1)$$

$Z_j =$ the predicted value at pixel j,
$Z_i =$ the measured value at point i,
$d_{ij} =$ distance between pixel j and point i.

We used a quadratic distance weighting model because it reduces the influence of distant points on prediction. For each spatial data set, we randomly selected 10% of the point observations to use for

interpolation. Subsetting the data improved computer processing time and allowed us to account for spatial and temporal autocorrelation among successive observations. Concentrations were estimated at 988 pixels in a 200-m grid pattern using the "idw" function in the R package "gstat" (Pebesma, 2004). We selected this grid size following guidelines provided in Hengl (2006), where resolution should be based on the spatial arrangement of point observations, the areal extent, and computer processing time. This pixel size also aligns with the spatial resolution of our point measurements (see above). Daily concentrations were then modeled through time by linearly interpolating between sample dates at each pixel, producing daily CO_2 and CH_4 estimates at 988 locations across the lake surface for the majority of ice-free period (249 days).

In addition to producing daily maps of CO_2 and CH_4 concentration, we also generated spatially explicit estimates of k and diffusive flux ($Flux_D$) to the atmosphere. We modeled $Flux_D$ according to

$$\mathrm{Flux}_D = \left(\mathrm{C_{aq}} - \mathrm{C_{eq}}\right) \times \mathrm{k}, \tag{2}$$

C_{aq} = surface water concentration,
C_{eq} = theoretrical concentration when in equilibrium with the atmosphere,
k = gas transfer velocity.

We calculated C_{eq} using water temperature, barometric pressure, and the atmospheric partial pressures of CO_2 and CH_4. We estimated k at 988 pixels (i.e., the same grid as above) at daily time steps using wind observations recorded at the buoy (lter.limnology.wisc.edu) and the spatially explicit k model provided in Vachon and Prairie (2013):

$$k_{600_{jl}} = 2.13 + 2.18 \times U_{10_l} + 0.82 \times U_{10_l} \times \log_{10}\left(fetch_{jl}\right), \tag{3}$$

$k_{600\ jl}$ = gas transfer velocity standardized at a Schmi dt number of 600 at pixel j *on day* l,
U_{10l} = average wind speed at a height of 10 m above the lake sureface on day l,
$fetch_{jl}$ = horizontal distance from the center of pixel j nearest shoreline in the upwind direction on day l.

The k model was derived empirically from 64 independent flux chamber measurements made in nine Canadian lakes ranging in surface area from 0.19 to 602 km^2 (Vachon & Prairie, 2013). Wind speed was converted to U_{10} based on common exponential wind profile assumptions using the R package "LakeMetabolizer" (Winslow et al., 2016). We calculated daily and annual average wind direction using the circular statistics R package "circular" (Agostinelli & Lund, 2017). We calculated *fetch* distance for each pixel and day using the daily average wind direction and lake shoreline shapefile using the R package "waver" (Marchand & Gill, 2018). We converted k_{600} to k for each gas using water temperature and Schmidt model coefficients provided in Raymond et al. (2012). Lastly, $Flux_d$ was calculated according to equation (2) for each pixel and day to produce spatially explicit efflux estimates through the majority of the lake's ice-free period.

2.4. Lake Center Versus Lakewide Estimates

To assess representativeness of sampling sites at the lake center, we compared lakewide concentration and flux estimates to those at the buoy. For the lakewide values, we summarized the spatially weighted distributions from the 988 pixel estimates. We calculated the daily mean, median, interquartile range ($Q_{25\text{-}75}$), and the inner 90th percentile range ($Q_{5\text{-}95}$); the latter being the difference between the 95th and 5th percentiles. To represent the lake center, we did not use the observed conditions at the buoy preceding and succeeding the FLAMe surveys (see above). Rather, daily concentrations and fluxes were calculated by averaging the modeled values for the 9 pixels (3 × 3 grid) surrounding the buoy location. These buoy estimates align temporally with the lakewide estimates and incorporate daily fluctuations in flux attributable to wind. The percent differences between the estimated values at the buoy (X_{buoy}) and the lakewide mean (X_{spatial}) were calculated as

$$\%\text{Difference} = 100\times\frac{\text{abs}\left(X_{\text{buoy}}-X_{\text{spatial}}\right)}{\left(X_{\text{buoy}}+X_{\text{spatial}}\right)/2} \quad (4)$$

Because some of our buoy and lakewide values are extremely close to zero and many CO_2 fluxes are negative, we report the median percent difference over the study period.

3. Results

Lake Mendota experienced typical weather and lake conditions in the year of our study. Air temperature and precipitation were similar to the 40-year averages (http://www.aos.wisc.edu/~sco/clim-history/7cities/madison.html). Water temperature and the phytoplankton community followed the typical seasonal phenology (Carey et al., 2016). Thermal stratification lasted from mid-May to early November (Figure 2). Although cyanobacteria comprised the majority of the phytoplankton biovolume in 2016 (lter.limnology.wisc.edu), no large cyanobacteria blooms occurred.

3.1. Temporal Concentration Patterns

Surface concentrations of CO_2 and CH_4 varied substantially through time. CO_2 concentrations ranged between 6.8 and 184.3 μM (0.37 to 11.65 saturation ratio). The mean of daily means (i.e., grand mean) and the median of daily medians (i.e., grand median) were 19.8 and 14.8 μM, respectively. These "grand" metrics account for both temporal and spatial heterogeneity. CO_2 saturation ratios ranged between 0.37 and 11.65 with a grand mean and grand median of 1.08 and 0.86, respectively. Due to seasonal changes in water temperatures, the concentration of CO_2 in equilibrium with the atmosphere fluctuated between 13.1 and 25.4 μM. Temporally, CO_2 was usually undersaturated during the summer stratified months but became highly supersaturated during fall turnover (Figure 2).

For CH_4, Lake Mendota was almost exclusively supersaturated relative to the atmosphere (Figure 2). CH_4 concentrations ranged between 0.002 and 5.36 μM, with a grand mean and grand median of 0.29 and 0.16 μM, respectively. Theoretical CH_4 concentrations in equilibrium with the atmosphere varied between 0.0027 and 0.0042 μM. Hence, CH_4 was on average 97.8 times supersaturated relative to the atmosphere (range of 0.48 to 2,786 saturation ratio). Temporally, CH_4 was higher in the late summer and increased during fall mixis (Figure 2).

3.2. Spatial Concentration Patterns

The spatial patterns of CO_2 and CH_4 concentrations and their relative spatial heterogeneity changed over the year. During spring and summer, lake locations near river inlets often had elevated concentrations of one or both gases compared to offshore waters (Figure 3). Spatial variability was low for CO_2 during the stratified period but variability (and concentration) increased substantially during fall turnover (Figures 2 and 3). At this time, a large CO_2 gradient emerged across the lake surface with greater concentrations in the western half of the lake (Figure 3). Although CH_4 also increased during turnover, the spatial patterns did not match CO_2. During the stratified period, CH_4 was lowest in the lake center and elevated in the northern bay (Figure 3). During fall turnover, the location of highest CH_4 shifted, and the spatial pattern became patchier. In late September the northeastern bay had higher concentrations, and in early November, patches of CH_4-enriched water occurred in the middle of the lake (Figure 3).

Comparatively, CH_4 concentrations were more spatially heterogeneous than CO_2 concentrations (Figure 3). The average coefficient of variation among sample dates for CO_2 was 0.12, whereas the mean coefficient of variation for CH_4 was 0.65 (Table 1). For CO_2 concentration, the $Q_{5\text{-}95}$ averaged 5.3 μM over the study period, meaning that on average, 90% of the lake surface was within a concentration range of 5.3 μM. For CH_4 concentration, the $Q_{5\text{-}95}$ averaged 0.42 μM among dates. Placing these ranges in the context of the mean concentrations, we point out that the average $Q_{5\text{-}95}$ of CH_4 was 145% of the grand mean CH_4, whereas the average $Q_{5\text{-}95}$ of CO_2 was only 27% the grand mean CO_2 (Table 1), indicating that CH_4 was generally more spatially heterogeneous than CO_2.

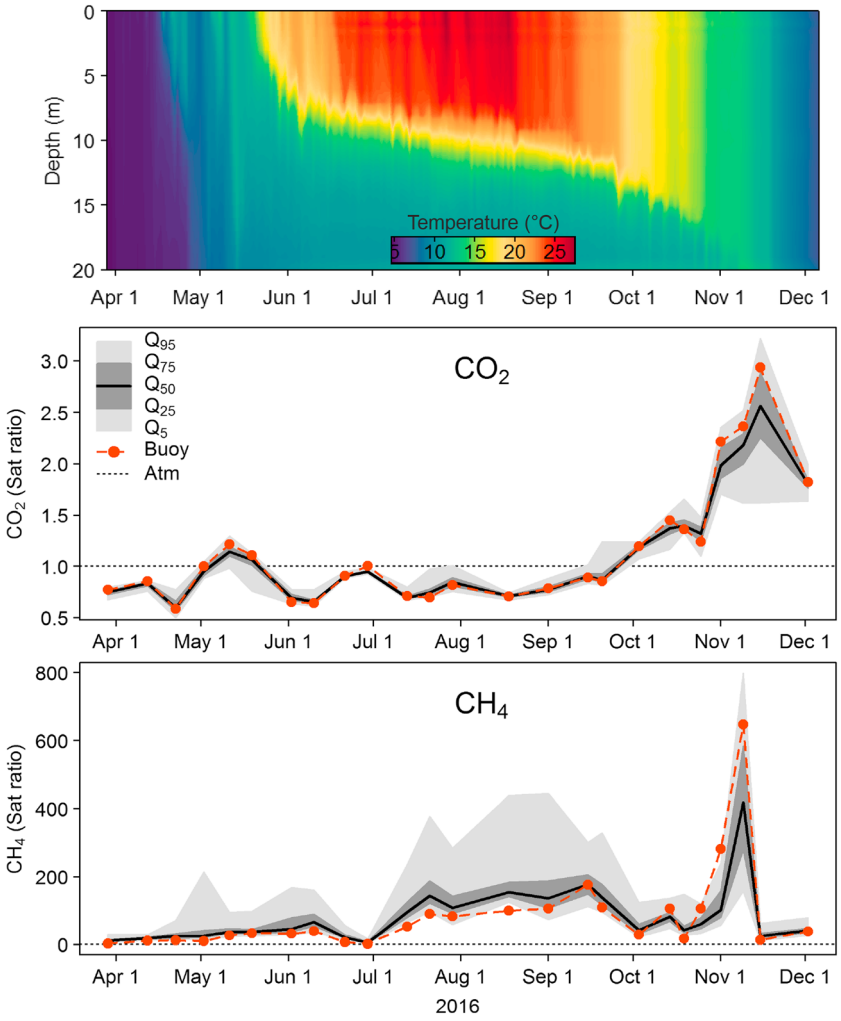

Figure 2. Seasonality of water temperature (upper panel), CO_2 (middle panel), and CH_4 (lower panel) concentrations. Gray polygons depict rolling boxplots of the spatial distribution of gas concentrations through time. A saturation ratio (sat ratio) of 1 is in equilibrium with the atmosphere (dotted line). The orange circles are the concentrations at the buoy located near the lake center.

3.3. Gas Transfer Velocity

Differences in wind speed and direction drove variation in *k* through time and across the lake surface. Wind speeds averaged 4.1 m/s, and wind direction averaged a bearing of 254° (WSW; Figure 4), but all wind directions occurred. Overall, the lake's geographic center had larger annual estimates of *k* than the lake edges. Differences in *k* among nearshore areas reflected the frequency of wind direction. The southern and western shores were more frequently upwind, resulting in shorter *fetch* distances and lower annual *k* estimates.

3.4. Flux

In general, the temporal patterns in fluxes (Figure 5) tracked the seasonal patterns in concentrations (Figure 2). The added day-to-day variability in flux was attributable to variation in wind and its modeled effect on *k*. During summer months, the mean CO_2 efflux across the lake surface was negative, indicating that the lake was taking in CO_2 from the atmosphere. However, during mixis, CO_2 efflux became positive and increased substantially. Our estimates of CO_2 efflux ranged between −43.3 and 687.0 mmol·m^{-2}·day^{-1}. The grand mean and grand median CO_2 efflux were 8.0 and −4.5 mmol·m^{-2}·day^{-1}, respectively. Of the 246,012 individual estimates (i.e., 988 pixels X 249 days), 65% indicated negative efflux (i.e., flux into

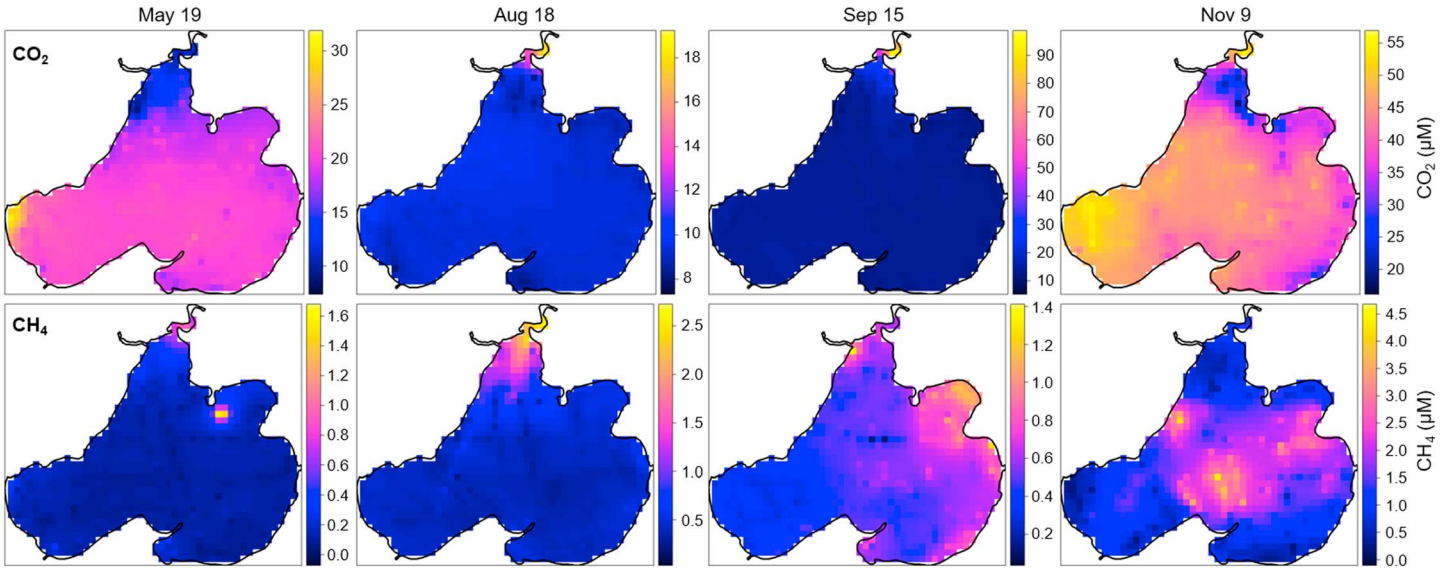

Figure 3. Spatial patterns of CO_2 (upper panels) and CH_4 (lower panels) on four dates representing spring, summer, start of turnover, and end of turnover. Concentrations were predicted at a 200-m grid. Each panel was plotted with a unique color ramp to highlight the spatial pattern on each day.

the lake). Thus, the flux of CO_2 was more frequently into Lake Mendota, but the lake was a net CO_2 source over the entire open water period, primarily due to the large efflux during autumn.

Throughout the entire open water period, Lake Mendota continually emitted CH_4 to the atmosphere. The range in CH_4 efflux was −0.001 to 24.51 mmol·m^{-2}·day^{-1}, with a grand mean of 0.93 mmol·m^{-2}·day^{-1} and a grand median of 0.56 mmol·m^{-2}·day^{-1}. Only four individual estimates indicated flux of CH_4 from the atmosphere into the lake, while the vast majority (n = 246,008) signified positive efflux. The greatest CH_4 efflux rates occurred during the warm summer months and fall turnover (Figure 5) when concentrations were elevated across the lake surface.

The spatial patterns of diffusive fluxes mimicked the heterogeneity observed in concentrations. Spatially, the highest CO_2 fluxes and concentrations occurred adjacent to river inlets and in the lake's western basin (Figure 6). Lower fluxes occurred in an arc along the lake's northern and eastern shores, and the annual efflux was negative for two pixels located in the river-lake transition zone of the northern bay. For CH_4, the northern bay had higher annual efflux estimates (1.4 to 3.5 mmol·m^{-2}·day^{-1}) while the center of the lake was low (0.85 mmol·m^{-2}·day^{-1}; Figure 6).

3.5. Lake Center Versus Lakewide Cumulative Flux

The cumulative efflux of CO_2 and CH_4 from Lake Mendota over the open water period was positive, indicating that on the annual scale the lake was a net source of both gases to the atmosphere. Cumulative CO_2

Table 1
Concentration and Flux Summary

		Unit	Spatial mean	CV mean	$Q_{5\text{-}95}$ mean	Buoy mean	Median % Difference between lake center and spatial estimates
CO_2	Concentration	μM	19.81	0.12	5.3	20.07	4.6%
	Flux	mmol·m^{-2}·day^{-1}	8.04	—	18.9	9.76	20.2%
CH_4	Concentration	μM	0.29	0.65	0.42	0.25	44.9%
	Flux	mmol·m^{-2}·d·$^{-1}$	0.93	0.61[a]	1.36	0.85	37.9%

Note. CV = coefficient of variation. Spatial mean is the average value across the lake surface over the open water period (249 days). CV and $Q_{5\text{-}95}$ were computed for each day and averaged. Buoy mean is the average daily value at the lake center. Percent difference was computed between buoy and spatial estimates for each day, and we report the median percent difference because distributions are nonnormal. "—" means unable to calculate CV for CO_2 flux because some fluxes were negative.
[a]CV for CH_4 flux calculated after omitting four negative flux estimates.

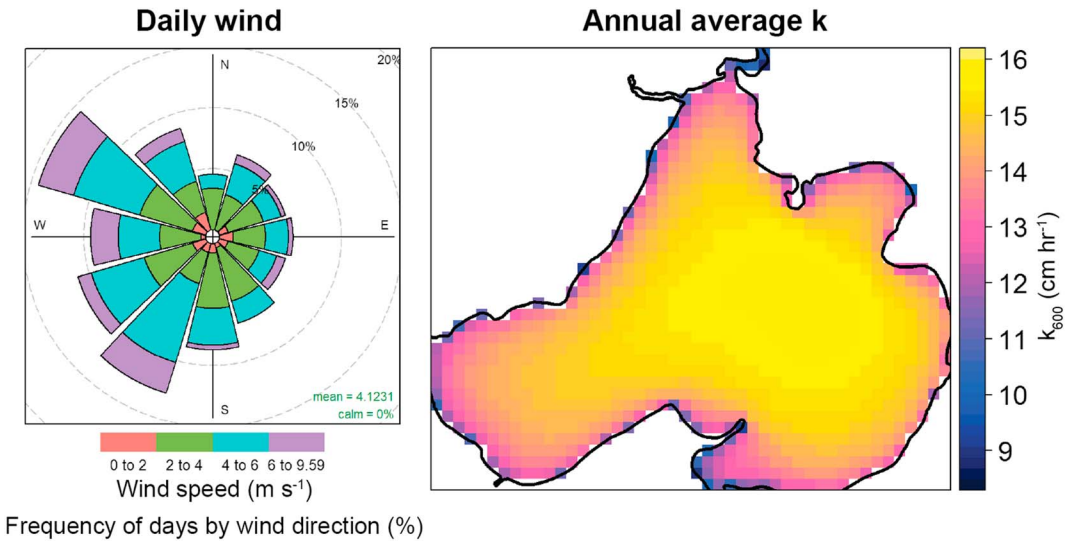

Figure 4. Daily wind conditions (left) and annual average gas transfer velocities (k; right). High frequency wind data from the buoy were used to compute daily average wind speed and direction. Daily wind was used to estimate k_{600} at 988 discrete pixels, which were averaged through time to produce the map of annual average k_{600}.

efflux was negative from March to October but became positive in November (Figure 7) associated with a substantial increase in surface concentration during mixis (Figure 2). Despite functioning as a CO_2 sink for the majority of the year, the positive CO_2 efflux rates in fall were large enough to switch the lake to a net source on the annual scale. The cumulative efflux of CH_4 was always positive and continually increased (Figure 7). The molar ratio between cumulative CO_2 and CH_4 flux was 8.7 (i.e., 8.7 mol of CO_2 emitted per mol of CH_4).

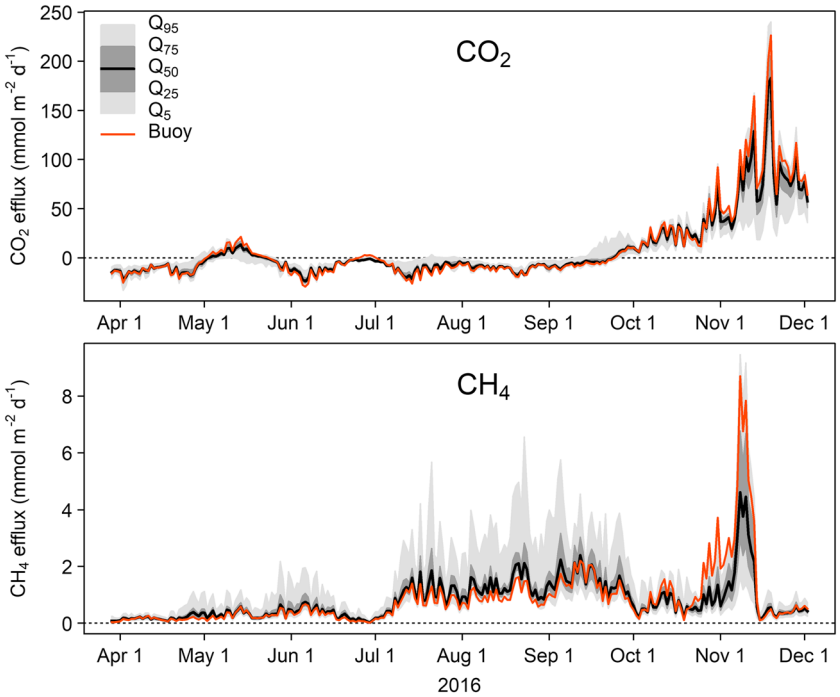

Figure 5. Spatial and temporal variability in CO_2 and CH_4 efflux. Gray polygons depict a rolling boxplot of the spatial distribution of fluxes through time. Orange line indicates the flux estimated at the buoy. Positive values indicate diffusive flux from the lake to the atmosphere. Dashed line indicates zero flux.

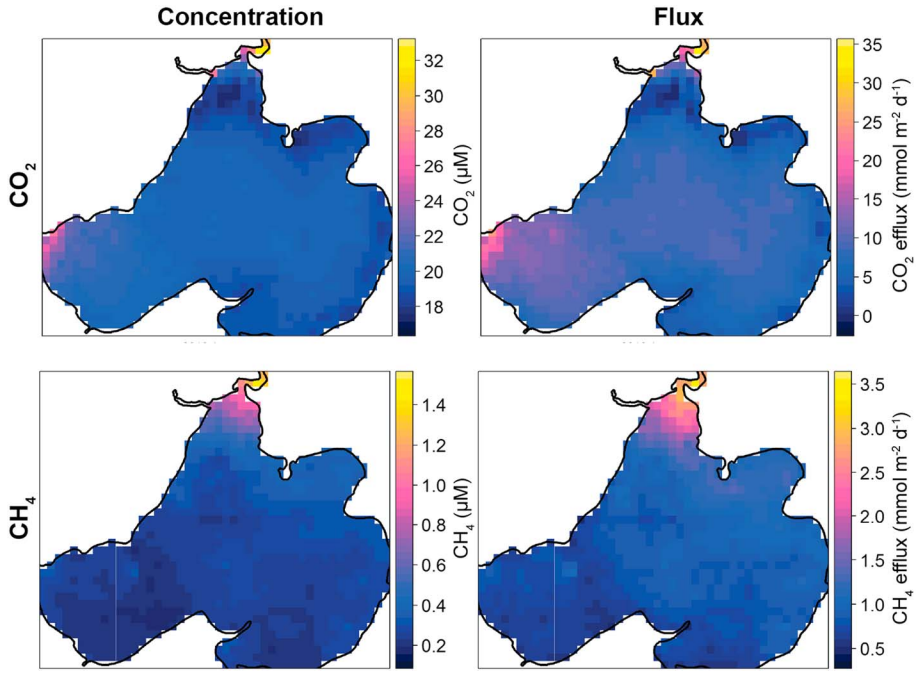

Figure 6. Annual average concentration (left panels) and diffusive efflux (right panels) across the lake surface. Each pixel is the average daily estimate for that pixel between 29 March and 2 December 2016.

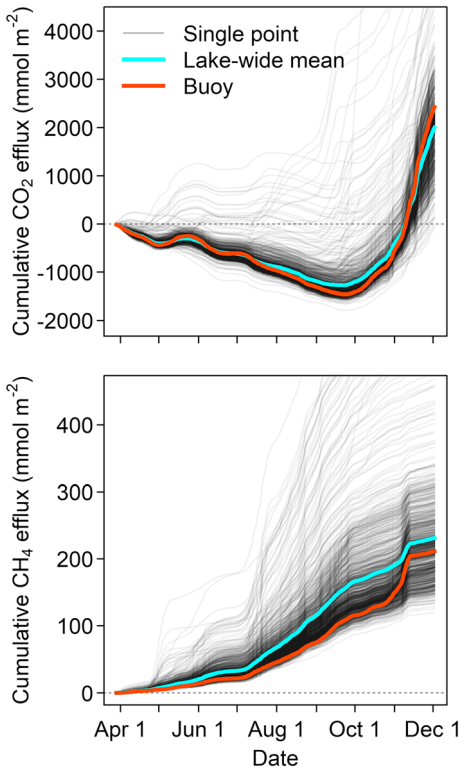

Figure 7. Cumulative CO_2 (upper panel) and CH_4 (lower panel) diffusive efflux from Lake Mendota to the atmosphere. Flux estimates are plotted for the lakewide mean (cyan), the buoy site (red), and the 988 individual pixels (light gray). Dotted horizontal line indicates zero net flux. The *y* axes were truncated to improve data visualization.

Flux estimates that incorporated spatial heterogeneity differed from estimates based on conditions at the central buoy. Across the entire lake surface, we estimated that over 249 days (29 March to 2 December), Lake Mendota emitted 79.9 Mmol of CO_2 to the atmosphere. Using only the conditions at the buoy, the total efflux CO_2 estimate would have been 97.0 Mmol. Comparatively, both CO_2 flux estimates followed similar temporal trends, but the buoy had a larger magnitude in both directions (Figure 7). Over the open water period, the median percent difference between the buoy and the lakewide CO_2 flux estimate was 20.2% and was larger than the median percent difference in CO_2 concentration (4.6%; Table 1). For CH_4, the median percent differences between the buoy and spatial estimates for concentration and flux were 44.9% and 37.9%, respectively. Lake Mendota emitted 9.23 Mmol of CH_4 annually based on conditions across the entire lake surface, while the estimate at the buoy was 8.44 Mmol of CH_4. Although the annual CH_4 estimates were comparable, the daily flux rate at the buoy included both types of extremes (i.e., lower fluxes during summer and higher fluxes during fall turnover), leading to a convergence with the lakewide cumulative estimate (Figure 7).

4. Discussion

Concentrations and fluxes of CO_2 and CH_4 varied in time and space. River inlets, variation in carbon processing, physical mixing, and wind dynamics all appeared to influence patterns of both gases. Flux patterns of each gas largely mirrored dissolved gas concentration patterns; however, spatial variability in *k* made the lake center contributes disproportionately to total flux across the lake surface. For Lake Mendota, portraying the entire lake surface with observations at the lake center was reasonable

for CO_2 concentration. However, this location was less representative for CO_2 flux (compared to CO_2 concentration) as the lake center overestimated annual emissions by 21%. Thus, in Lake Mendota, combining a single monitoring station with a spatially explicit flux model would adequately portray CO_2 fluxes over the whole lake during the stratified period. For CH_4, the lake center was a reasonable representation of lakewide diffusive efflux, as it underestimated the annual CH_4 efflux by 8.6%. However, the buoy estimate would have been substantially worse had it not been fortuitously positioned within a patch of CH_4-enriched water during mixis. The lake center poorly represented the daily lakewide concentration and flux likely due to the spatial heterogeneity in CH_4 sources (Bastviken et al., 2008) and transport to the lake surface (DelSontro, del Giorgio, & Prairie, 2018). These results suggest that spatial evaluations in other lakes are needed to validate the uncertainties with using single-point samples to represent lakewide processes. Rather than assuming spatial homogeneity, future investigations and scaling-up exercises should acknowledge the uncertainty with extrapolating from spatially limited data sets.

4.1. Temporal Patterns

Fluxes of CO_2 in Lake Mendota followed similar seasonal trends as other productive, dimictic lakes (Bartosiewicz et al., 2015; Casper et al., 2000; Maberly, 1996). For most of the stratified period, the net flux of CO_2 was into the lake (Figure 5). At the same time, dissolved oxygen at the lake surface was highly supersaturated and negatively correlated with CO_2 (Figures S2 and S3), suggesting metabolic control of CO_2. This undersaturated CO_2 state concluded in late September as surface waters cooled and the surface mixed layer deepened (Figure 2), which likely entrained CO_2-rich hypolimnetic waters (Ducharme-Riel et al., 2015). The hypolimnion of Lake Mendota typically becomes anoxic and supersaturated with CO_2 during the summer months (Hart et al., 2017), leading to elevated CO_2 surface concentrations and efflux to the atmosphere during fall turnover (Figure 5; Reed et al., 2018). While phytoplankton abundance can increase during turnover due to delivery of hypolimnetic nutrients (Sommer et al., 1986, 2012), any increase in primary production or CO_2 uptake that may have occurred was clearly overwhelmed by the large supply of hypolimnetic CO_2, resulting in a large and prolonged (2 to 3 months) off-gassing event.

While this autumnal spike in CO_2 has been well documented in temperate lakes and reservoirs (Ducharme-Riel et al., 2015; Jones et al., 2016), we were surprised by the lack of CO_2 efflux at ice break. On 29 March 2016 (16 days after ice break), CO_2 concentrations were undersaturated (Figure 2). Lakes in temperate and boreal zones commonly have elevated CO_2 concentrations and large off-gassing events following ice break (Ducharme-Riel et al., 2015; Karlsson et al., 2013; Striegl et al., 2001) due to underice respiration. While we did not sample CO_2 during the winter immediately prior to our study, we measured concentrations the prior winter on five dates surrounding ice break. CO_2 concentrations on the day of ice break were near saturation (32 μM; 109% saturation) despite being 240% saturation 26 days prior (Table S1). We suspect that in Lake Mendota (and other productive, ice-covered lakes), underice primary production lowers CO_2 concentrations in the final weeks of ice cover, supplanting the underice CO_2 accumulation. Phytoplankton densities can increase by 2 to 3 orders of magnitude to reach or even exceed summertime levels in the weeks preceding ice break when phosphorus concentrations are high and sufficient light is passing through the thinning ice/snow layer (Salmi & Salonen, 2016). We have observed elevated underice phosphorus concentrations and diatom blooms prior to ice break (Center for Limnology NTL-LTER, 2007; Lead et al., 2010), supporting the hypothesis of CO_2 uptake by primary producers during this late winter period. Besides this lack of CO_2 efflux at ice break, CO_2 followed expected temporal patterns for productive lakes.

As with CO_2, seasonal patterns in CH_4 were similar to other productive lakes (Bartosiewicz et al., 2015; Casper et al., 2000), following typical phenologies in temperature and stratification. The large increase in CH_4 concentrations and fluxes in November was presumably due to mixing of CH_4-enriched hypolimnetic water (Harrits & Hanson, 1980; Juutinen et al., 2009; Rudd & Hamilton, 1978). Despite lasting only 2 weeks, this autumnal off-gassing event was responsible for 15% of CH_4 emitted to the atmosphere during the 249 day study. Compared to CO_2, this elevated CH_4 state was short-lived, as concentrations declined within approximately 1 week of vertically isothermal conditions. The combination of microbial oxidation (Bastviken et al., 2008; Fallon et al., 1980; Kankaala et al., 2007; Rudd & Hamilton, 1978) and rapid efflux to the atmosphere likely drove CH_4 concentrations down after turnover, leading to the brief CH_4 spike in November. The higher CH_4 concentrations and fluxes in late summer likely reflected increased

production under warmer water temperatures (Rasilo et al., 2015; Yvon-Durocher et al., 2014; Zeikus & Winfrey, 1976) and the expansion of anoxia in the hypolimnion and sediments (Juutinen et al., 2009; Winfrey & Zeikus, 1979). While oxidation may also have been elevated in summer due to its temperature optima (Harrits & Hanson, 1980), the production of CH_4 in oxic (Bogard et al., 2014) or nearby anoxic environments (Hofmann, 2013) and the delivery of CH_4 to the surface (DelSontro, del Giorgio, & Prairie, 2018) was sufficient to keep the lake continually off-gassing CH_4 year-round.

Lake Mendota gas concentrations and fluxes were within expected ranges for large, eutrophic lakes. Compared to a recent global synthesis (Holgerson & Raymond, 2016), Lake Mendota's CO_2 concentrations and fluxes were lower than for lakes of similar size, likely due to the lake's eutrophic status. In general, productive lakes are more frequently CO_2 undersaturated (Balmer & Downing, 2011) driven by low concentrations during summer stratified periods (Bartosiewicz et al., 2015; Maberly, 1996). Similarly, seasonal CO_2 variability was pronounced, consistent with other studies of nutrient-rich, temperate lakes (Maberly et al., 2013). For CH_4, Lake Mendota had higher concentrations and fluxes than lakes of similar size (Holgerson & Raymond, 2016), again likely due to the lake's eutrophic status. Productivity (Huttunen et al., 2003; Juutinen et al., 2009) and chlorophyll (DelSontro, Beaulieu, & Downing, 2018) have been linked with higher CH_4 concentrations and fluxes in lakes. Lake Mendota emitted 8.7 moles of CO_2 for every mole of CH_4, which is 1 to 2 orders of magnitude lower than lakes of similar size (Holgerson & Raymond, 2016). In this context, Lake Mendota emitted a substantially large proportion of its carbon to the atmosphere as CH_4. With eutrophication, lakes may shift a greater proportion of their carbon cycling toward CH_4 (DelSontro, Beaulieu, & Downing, 2018; Moss, 2011), altering the contribution of lakes to global greenhouse gas budgets.

4.2. Spatial Patterns

Spatial patterns for each gas remained relatively consistent throughout the stratified period but changed substantially during fall mixing. CO_2 concentrations were fairly uniform across much of the lake surface during the stratified period, suggesting consistent lakewide drivers. While phytoplankton distribution can exhibit high spatial heterogeneity (George & Edwards, 1976; Rinke et al., 2009), which we observed at some times of the year (Figure S8), in Lake Mendota their effect on the spatial pattern of CO_2 concentration during stratification appears limited.

Spatial uniformity of CO_2 concentration may be due to carbonate chemistry. Lake Mendota is an alkaline (~3,600 μeq/L) lake characterized by high dissolved inorganic carbon (DIC) concentrations (~44 mg C/L) and pH (~8.4). Thus, CO_2 comprises a small fraction (~1%) of the total DIC pool. In alkaline systems, carbonate chemistry dampens the effect of metabolism on CO_2 variability (Peeters et al., 2016) and increases the time needed for CO_2 to equilibrate with the atmosphere (Stets et al., 2017). For example, in a German lake with a similar alkalinity as Lake Mendota (DIC ~35 mg C/L, pH ~8.5), metabolically driven diel changes in CO_2 were roughly 20% of DIC and dissolved oxygen (Peeters et al., 2016). Conversely, we expect greater spatial (and temporal) variability in low alkalinity systems. Consistent with this prediction, Crawford et al. (2015) found a 1,000 ppm (~40 μM) range in CO_2 concentrations across the lake surface in a low-alkalinity lake (pH ~4.5) in Northern Wisconsin, and CO_2 varied by ~500 μtam (~20 μM) across the lake surface of a moderately alkaline Swedish lake (pH ~ 6.2; Natchimuthu et al., 2017). Comparatively, the average CO_2 $Q_{5\text{-}95}$ across Lake Mendota was only 5.3 μM and was smaller during the summer months when pH (Figure S2) and carbonate buffering capacity were greatest. In low-alkalinity systems, CO_2 and DIC concentrations are nearly equivalent (Stets et al., 2017), allowing metabolic processes and gas exchange to directly alter CO_2 concentrations. Spatial heterogeneity in CO_2 concentration varies within and among lakes, shaped in part by the magnitude and variability of biological processing and the carbonate buffering capacity of the system.

While overall CO_2 spatial variability was low, clear spatial patterns of CO_2 existed across Lake Mendota that would have been missed had sampling only occurred in the lake's geographic center. The northern bay of Lake Mendota receives direct inputs of nutrient-rich water, and we observed an unusual pattern for CO_2 here. The lowest average CO_2 concentrations occurred in the river-lake transition zone, and some portions of the bay were identified as CO_2 sinks (Figure 6). Undersaturated CO_2 in the transition zone needs to be accredited to biological processing, as all potential hydrologic sources had higher CO_2. This nutrient-rich transition zone routinely had high algal fluorescence and supersaturated oxygen concentrations

(Figure S7), suggesting high primary production. River inlets are notable sites for metabolic processing in lakes as these locations receive and process material from the upstream network (Mackay, Jones, Folkard, & Thackeray, 2011; Makarewicz et al., 2012; Wynne & Stumpf, 2015) before it mixes into the lake proper. While this zone made a small overall contribution to CO_2 flux in this large lake, the effect of river inlet habitats on whole lake dynamics could potentially be substantial in other lakes, depending on site-specific hydrologic and biological conditions.

We also witnessed a CO_2 spatial anomaly during turnover that has rarely been documented (but see Natchimuthu et al., 2017). There was a lakewide gradient of CO_2 concentration (Figure 3), mirroring the spatial patterns of other metabolic variables. Lower CO_2, higher dissolved oxygen, and higher phycocyanin (an indicator of cyanobacteria) occurred on the downwind side of the lake (Figure S8). We postulate that wind blowing across the lake surface drove buoyant material (including cyanobacteria) and surface water downwind and caused upwelling of deeper water on the lake's upwind side. This "conveyer belt" circulation pattern has been shown to drive horizontal spatial patterns of phytoplankton in a variety of lakes and reservoirs (Blukacz et al., 2009; George & Edwards, 1976; Mackay, Jones, Thackeray, & Folkard, 2011) and CO_2 in a small Swedish lake (Natchimuthu et al., 2017). We witnessed similar spatial gradients in CO_2 concentration in November of 2014 and 2017 (Figure S9), suggesting this turnover mixing dynamic may be a regular phenomenon in Lake Mendota. The emergence of this CO_2 gradient will be dependent on the prevailing wind (speed, direction, and duration), the vertical CO_2 concentration gradient, and the abundance and buoyancy of the algae species present. In this lake, the upwind-downwind gradient in CO_2 concentration during turnover was the largest source of variability in both space and time, and thus, sampling along this gradient in other lakes may be critical to accurately estimate total CO_2 exchange with the atmosphere.

CH_4 was more heterogeneous than CO_2 across the lake surface. The northern bay of the lake routinely had the highest CH_4 concentrations and fluxes, presumably due to river inputs and/or CH_4 production in littoral sediments. River inlets are frequently sites of elevated CH_4 in lakes and reservoirs (Delsontro et al., 2011; Natchimuthu et al., 2016), so sampling these areas is required for accurate lakewide emission estimates (Beaulieu et al., 2016). On most sampling dates, we observed a conductivity gradient from the Yahara River inlet through the northern bay (Figure S7), indicating an allochthonous water source that could have delivered CH_4 to the river-lake transition zone. Additionally, CH_4 may have been produced within the bay itself, as it is an expansive, shallow basin where alluvial sediments accumulate. CH_4 production may be further enhanced in the river-lake transition zone due to increased phytoplankton density and sedimentation of fresh organic matter, which can fuel methanogenesis and other respiratory processes (Grasset et al., 2018; West et al., 2012). Across all observations, CH_4 concentrations were positively correlated with algal fluorescence; however, all regression models explained very little of the total variance (Figure S4). Higher chlorophyll and primary productivity have been linked to higher CH_4 production (Bogard et al., 2014; West et al., 2016), concentrations (Juutinen et al., 2009), and fluxes to the atmosphere (Casper et al., 2000; DelSontro, Beaulieu, & Downing, 2018). Despite the limited variance of the regression models, we suggest that phytoplankton heterogeneity shapes at least some of the spatial variation in CH_4. In considering the spatial heterogeneity of CH_4, shallow littoral habitats (Hofmann, 2013) and river-lake transition zones (Delsontro et al., 2011; Natchimuthu et al., 2016) are especially important for lakewide CH_4 dynamics. The direct emissions to the atmosphere from these habitats are missed with pelagic-only sampling surveys, leading to underestimation of CH_4 emissions from lentic waterbodies (Paranaíba et al., 2018; Wik et al., 2016).

Similar to CO_2, the spatial arrangement of CH_4 changed during fall turnover, though the location of maximum concentrations differed. At the culmination of turnover, the lake's central basin became extremely saturated with CH_4 (Figure 3) as the lake became isothermal. Most likely, vertical advection of the CH_4-enriched hypolimnion caused concentrations to increase above the deeper parts of the lake. The patchy CH_4 appearance may have aligned with distinct upwelling and downwelling flowpaths. However, at odds to this hypothesis, the spatial patterns of CO_2 and CH_4 did not match. We propose entrainment of the hypolimnion increased surface concentrations of both gases, but enrichments were mediated by gas-specific processes. For CO_2, metabolism appeared to have differed spatially, as lower CO_2 occurred in locations with elevated dissolved oxygen and phytoplankton densities (Figure S8). The CO_2 pattern also reflected carbonate buffering, which could have eroded the fine-scale patchiness associated with heterogeneous vertical mixing. For CH_4, oxidation and dissolution of bubbles may have played roles in the development of the CH_4 pattern. CH_4 oxidation often increases

during turnover, which can be responsible for upward of 90% of the CH_4 accumulated in the hypolimnion (Fallon et al., 1980; Kankaala et al., 2007). Ebullition is highly spatially heterogeneous in lakes (Delsontro et al., 2011), and increased water velocities along profundal sediment-water interfaces may have elicited bubble release and dissolution in the water column (Murase et al., 2005). The specific locations of elevated CH_4 during turnover varied among years (Figure S9), suggesting at least one stochastic process aided in the formation of the CH_4 spatial pattern at the lake surface. While the underlying mechanisms for the elevated CH_4 condition at the lake center are unverified, our results revealed the extremely variable nature of CH_4 during turnover. By sampling intensively across space and through time, were we able to witness this unexpected spatial pattern that may commonly occur in lakes that routinely mix. The patchy nature of CH_4 and the spatial mismatch between CO_2 and CH_4 emphasizes the difficulty in accurately quantify fluxes during turnover. Mixing events are periods of chaotic water movements that may stimulate biological activity and are critical to account for in whole lake biogeochemical budgets.

4.3. Gas Transfer Velocity

Although flux estimates largely mirrored concentration patterns, heterogeneity in k was important for flux calculations—especially at shorter time scales. Day-to-day differences in flux were attributable to differences in wind speeds through its modeled effect on k. For example, during 1 week in mid-November, Lake Mendota CO_2 efflux varied between 53 and 170 $mmol \cdot m^{-2} \cdot day^{-1}$ (Figure 5) entirely due to wind-driven variation in k. Spatially, wind direction dictated the spatial pattern of k on each day, enhancing flux rates on Lake Mendota's downwind side by 50% to 300% compared to the upwind side. At longer time scales (>weekly), the temporal and spatial variation in flux attributable to k averaged out, as the temporal and spatial flux patterns largely followed concentration. Thus, the flux rate at any given place or time is strongly influenced by k, but the effect k has on flux variability is most pronounced at shorter time scales, with one key exception (see below).

Spatial heterogeneity in k caused the center of Lake Mendota to contribute disproportionately to lakewide gas exchange. Because of the log-*fetch* relationship in the k model (Vachon & Prairie, 2013), spatial variation in k was most pronounced near the lake's upwind shore, and all locations beyond ~1 km from the upwind shore had relatively high k for that day. Because of Lake Mendota's large size, the central pelagic zone was consistently in a relatively turbulent, high-k environment regardless of wind direction. This nonlinear spatial relationship caused the annual average k in the lake center to be 50% to 100% greater than the lake margins (Figure 4). In other lakes, if calculations of k and flux are only made at the lake center, they may overestimate lakewide values, as they do not represent wind-sheltered portions of the lake.

Despite the effect k has on gas exchange rates, at the entire lake surface scale or to the annual scale, the range in concentrations was more important for flux determination in Lake Mendota (Figure S5). Fluxes of CO_2 and CH_4 had higher correlations with concentrations ($r \sim 0.9$) than k values ($r \sim 0.3$). We acknowledge that our k model is relatively simple and does not incorporate subdaily variation in wind, internal wave motions, nor thermal convection, which can significantly impact flux rates (Heiskanen et al., 2014; Podgrajsek et al., 2015; Read et al., 2012). In a comparable spatiotemporal study in Sweden, Natchimuthu et al. (2016, 2017) drew a similar conclusion that CO_2 and CH_4 concentrations were more important than k for describing gas efflux. Thus, variation in k is important when concentration ranges are small, but at larger temporal and spatial scales, the processes driving variability in concentrations become more important for emissions.

4.4. Lake Center Versus Lakewide

In general, the buoy followed the lakewide temporal CO_2 and CH_4 patterns, confirming its utility as an indicator of the lake as a whole. However, because of its geographic location, consistent biases in concentration and k lead to discrepancies in average concentration and total efflux from the lake. While the buoy CO_2 concentration generally aligned with the lakewide mean, spatial variability in k caused the buoy to have greater CO_2 influx during the summer months and greater efflux during autumn (Figure 7). To some extent, these two discrepancies counteracted each other at the annual scale. Despite comparable concentrations, the cumulative efflux estimate at the buoy was 27% larger than the spatially weighted estimate (Table 1). This divergence may be more substantial in lakes constantly supersaturated with CO_2 (as many lakes are), as greater CO_2 evasion rates would consistently occur offshore (e.g., Schilder et al., 2013). Further, many lakes have greater spatial heterogeneity in CO_2 concentration than Lake Mendota (e.g., Crawford et al., 2015;

Natchimuthu et al., 2017; Schilder et al., 2013), which combined with *k* variability may lead to substantial spatial variation in CO_2 flux and diminish the lakewide representativeness of a single location.

For CH_4, the buoy consistently disagreed with whole lake estimates. During the summer months, the buoy had lower concentrations and fluxes than the lakewide mean primarily due to the contribution of the lake's northern bay (Figure 6). This bay makes up only 4% of the total lake surface area but emitted over 10% of the CH_4 from the lake. Littoral areas and river-mouth habitats can contribute disproportionately to lakewide efflux (Natchimuthu et al., 2016; Paranaíba et al., 2018; Schilder et al., 2013; Wik et al., 2016) and are often missed using traditional sampling approaches (Wik et al., 2016). While the lake's northern littoral zone emitted a substantial amount of CH_4 during the summer, the lake center became highly CH_4-enriched during fall turnover and had the greatest daily rates of CH_4 efflux during this study. Had the buoy not fortuitously captured the large CH_4 off-gassing event during turnover (Figure 3), the buoy's cumulative efflux estimate would have been substantially lower than the lakewide mean. Over the ice-free period, the buoy only underestimated lakewide CH_4 efflux by 8.6%, but on any given day it poorly approximated the entire lake surface. In general, CH_4 fluxes are not well represented by a single location (Paranaíba et al., 2018; Wik et al., 2016), which needs to be acknowledged in individual lake carbon budgets as well as global syntheses of greenhouse gas emissions from lakes.

4.5. Study Limitations

Like all studies, our flux estimates include uncertainty and should not be considered as the exact amount of gas evaded from the lake. Physical and biological processes vary at distances shorter than our spatial resolution and at time scales shorter than our sample frequency. For example, diel patterns in light, metabolism, wind speeds, and temperature cause daily cycles in CO_2 (Peeters et al., 2016) and surface turbulence (MacIntyre et al., 1995; Podgrajsek et al., 2015). We sampled in the morning during time periods when CO_2 concentrations were elevated compared to the daily mean (Figure S6). Thus, we suspect our reported CO_2 concentrations and fluxes to slightly overestimate daily conditions. For CH_4, fluctuations in temperature and wind may contribute to variability in CH_4 production (Yvon-Durocher et al., 2014), oxidation (Harrits & Hanson, 1980), liberation from sediments (Bastviken et al., 2008; Hofmann et al., 2010), and entrainment from the hypolimnion (Erkkilä et al., 2018). Our study focused on diffusive flux, yet other flux types also contribute significant and often larger CH_4 emissions from lakes. For example, ebullition can contribute to over half of CH_4 efflux from lakes (Bastviken et al., 2004).

Although we account for spatial heterogeneity in *k* across the lack surface, our flux estimates relied on a relatively simple wind-based *k* model. We modeled *k* at daily time steps, rather than incorporating subdaily variability in wind speed and direction. Most empirically derived wind-based *k* models are nonlinear (e.g., Cole & Caraco, 1998). By averaging wind speed, we effectively dampen the effect wind gusts have on surface turbulence and likely underestimate gas exchange. Second, we ignored waterside surface convection, which tends to drive turbulence in small systems (Read et al., 2012) and at night (Podgrajsek et al., 2015). We likely underestimated *k* and exchange rates during times with increased internal wave motion or thermal convection (Heiskanen et al., 2014), such as fall turnover. Given the significance of the fall turnover period in determining annual emissions in this lake, we urge caution if our flux rates are used in a lake carbon budget. Despite model uncertainty and missing other processes and habitats that contribute to heterogeneity in gas emissions, our extensive spatial and temporal sampling revealed notable variation along these dimensions and provides a data-rich, comprehensive view of CO_2 and CH_4 surface dynamics in a single lake.

5. Conclusions

Physical and biological drivers of CO_2 and CH_4 act at multiple temporal and spatial scales, leading to heterogeneous carbon dynamics within individual lake ecosystems. This study highlights the dynamic nature of CO_2 and CH_4 in a single lake, showing that conditions can alternate between periods of uniformity to those of remarkable heterogeneity. Patterns of CO_2 and CH_4 were not always aligned, as each independently responded to a suite of physical and biogeochemical processes. These mechanisms do not always play out evenly across the lake nor are they static through time, leading to substantial heterogeneity that is often neglected in studies with limited temporal or spatial sampling designs. Spatially and temporally comprehensive data sets are rare in the literature, warranting future studies to determine if the patterns observed in this

lake are universal and the potential consequences they have on other ecosystem functions. Understanding the patterns, causes, and consequences of spatial heterogeneity in ecosystem function remains a frontier in ecology (Turner & Chapin, 2005), and by embracing spatial heterogeneity, we may be able to constrain the contribution of lakes to global carbon budgets and more generally improve our understanding of lake ecosystems.

Acknowledgments
Thanks to the many FLAMers for help with field sampling and system development. Thanks to the Bob Paulos, Terry Benson, and Barbara Birrittella at the Physical Sciences Lab for design and engineering of research equipment and support from a UW2020 award from the Wisconsin Alumni Research Foundation. Thanks to Matthew Bogard and other reviewers for providing feedback. L. C. L., P. J. S., A. R. D., and E. H. S. were supported by the North Temperate Lakes LTER program, NSF DEB-1440297. L. C. L. was partially funded through the U.S. Geological Survey's Watershed, Energy, and Biogeochemical Budgets program. J. T. C. was supported by the U.S. Geological Survey's Land Carbon program. P. S. was financially supported by the Austrian Science Fund (Vienna Doctoral Programme on Water Resource Systems, W 1219-N22) and the Vienna University of Technology (innovative project). Data are available at the NTL-LTER data portal (http://lter.limnology.wisc.edu https://doi.org/10.6073/pasta/fe9c5437f67254f521bf5f7e0308bf93), and models and code are available through github (github.com/lukeloken). Any use of trade, firm, or product names is for descriptive purposes only and does not imply endorsement by the U.S. Government.

References

Agostinelli, C., & Lund, U. (2017). R package "circular": Circular Statistics (version 0.4-93). Retrieved from https://r-forge.r-project.org/projects/circular/

Balmer, M., & Downing, J. (2011). Carbon dioxide concentrations in eutrophic lakes: Undersaturation implies atmospheric uptake. *Inland Waters*, *1*(2), 125–132. https://doi.org/10.5268/IW-1.2.366

Bartosiewicz, M., Laurion, I., & MacIntyre, S. (2015). Greenhouse gas emission and storage in a small shallow lake. *Hydrobiologia*, *757*(1), 101–115. https://doi.org/10.1007/s10750-015-2240-2

Bastviken, D., Cole, J., Pace, M., & Tranvik, L. (2004). Methane emissions from lakes: Dependence of lake characteristics, two regional assessments, and a global estimate. *Global Biogeochemical Cycles*, *18*, GB4009. https://doi.org/10.1029/2004GB002238

Bastviken, D., Cole, J. J., Pace, M. L., & Van de Bogert, M. C. (2008). Fates of methane from different lake habitats: Connecting whole-lake budgets and CH4 emissions. *Journal of Geophysical Research*, *113*, G02024. https://doi.org/10.1029/2007JG000608

Beaulieu, J. J., McManus, M. G., & Nietch, C. T. (2016). Estimates of reservoir methane emissions based on a spatially balanced probabilistic-survey. *Limnology and Oceanography*, *61*(S1), S27–S40. https://doi.org/10.1002/lno.10284

Blukacz, E. A., Shuter, B. J., & Sprules, W. G. (2009). Towards understanding the relationship between wind conditions and plankton patchiness. *Limnology and Oceanography*, *54*(5), 1530–1540. https://doi.org/10.4319/lo.2009.54.5.1530

Bogard, M. J., del Giorgio, P. A., Boutet, L., Chaves, M. C. G., Prairie, Y. T., Merante, A., & Derry, A. M. (2014). Oxic water column methanogenesis as a major component of aquatic CH4 fluxes. *Nature Communications*, *5*(1), 5350. https://doi.org/10.1038/ncomms6350

Brock, T. D. (1985). *A Eutrophic Lake: Lake Mendota, Wisconsin*. New York: Springer-Verlag. https://doi.org/10.1007/978-1-4419-8700-6

Butitta, V. L., Carpenter, S. R., Loken, L. C., & Pace, M. L. (2017). Spatial early warning signals in a lake maniuplation. *Ecosphere*, *8*(10). https://doi.org/10.1002/ecs2.1941

Carey, C. C., Hanson, P. C., Lathrop, R. C., & St. Amand, A. L. (2016). Using wavelet analyses to examine variability in phytoplankton seasonal succession and annual periodicity. *Journal of Plankton Research*, *38*(1), 27–40. https://doi.org/10.1093/plankt/fbv116

Casper, P., Maberly, S. C., Hall, G. H., & Finlay, B. J. (2000). Fluxes of methane and carbon dioxide from a small productive lake to the atmosphere. *Biogeochemistry*, *49*(1), 1–19. https://doi.org/10.1023/A:1006269900174

Center for Limnology NTL LTER. (2007). North temperate lakes LTER: Phytoplankton. Madison lakes area, 1995–current. https://doi.org/10.6073/pasta/3eb45259f93eb624759585c4649798b8

Cole, J. J., & Caraco, N. F. (1998). Atmospheric exchange of carbon dioxide in a low-wind oligotrophic lake measured by the addition of SF6. *Limnology and Oceanography*, *43*(4), 647–656. https://doi.org/10.4319/lo.1998.43.4.0647

Cole, J. J., Prairie, Y. T., Caraco, N. F., McDowell, W. H., Tranvik, L. J., Striegl, R. G., et al. (2007). Plumbing the global carbon cycle: Integrating inland waters into the terrestrial carbon budget. *Ecosystems*, *10*(1), 172–185. https://doi.org/10.1007/s10021-006-9013-8

Cooney, E. M., McKinney, P., Sterner, R., Small, G. E., & Minor, E. C. (2018). Tale of two storms: Impact of extreme rain events on the biogeochemistry of Lake Superior. *Journal of Geophysical Research: Biogeosciences*, *123*, 1719–1731. https://doi.org/10.1029/2017JG004216

Crawford, J. T., Loken, L. C., Casson, N. J., Smith, C., Stone, A. G., & Winslow, L. A. (2015). High-speed limnology: Using advanced sensors to investigate spatial variability in biogeochemistry and hydrology. *Environmental Science and Technology*, *49*(1), 442–450. https://doi.org/10.1021/es504773x

DelSontro, T., Beaulieu, J. J., & Downing, J. A. (2018). Greenhouse gas emissions from lakes and impoundments: Upscaling in the face of global change. *Limnology and Oceanography Letters*, *3*(3), 64–75. https://doi.org/10.1002/lol2.10073

DelSontro, T., del Giorgio, P. A., & Prairie, Y. T. (2018). No longer a paradox: The interaction between physical transport and biological processes explains the spatial distribution of surface water methane within and across lakes. *Ecosystems*, *21*(6), 1073–1087. https://doi.org/10.1007/s10021-017-0205-1

Delsontro, T., Kunz, M. J., Kempter, T., Alfred, W., Wehrli, B., & Senn, D. B. (2011). Spatial heterogeneity of methane ebullition in a large tropical reservoir. *Environmental Science & Technology*, *45*(23), 9866–9873. https://doi.org/10.1021/es2005545

Ducharme-Riel, V., Vachon, D., del Giorgio, P. A., & Prairie, Y. T. (2015). The relative contribution of winter under-ice and summer hypolimnetic CO2 accumulation to the annual CO2 emissions from northern lakes. *Ecosystems*, *18*(4), 547–559. https://doi.org/10.1007/s10021-015-9846-0

Erkkilä, K.-M., Ojala, A., Bastviken, D., Biermann, T., Heiskanen, J. J., Lindroth, A., et al. (2018). Methane and carbon dioxide fluxes over a lake: Comparison between eddy covariance, floating chambers and boundary layer method. *Biogeosciences*, *15*(2), 429–445. https://doi.org/10.5194/bg-15-429-2018

Fallon, R. D., Harrits, S., Hanson, R. S., & Brock, T. D. (1980). The role of methane in internal carbon cycling in Lake Mendota during summer stratification. *Limnology and Oceanography*, *25*(2), 357–360. https://doi.org/10.4319/lo.1980.25.2.0357

Fofonoff, N. P., Hayes, S. P., & Millard Jr, R. C. (1974). W.H.O.I./Brown CTD microprofiler: Methods of calibration and data handling. WHOI Tech. Rep., WHOI-74-89.

George, D. G., & Edwards, R. W. (1976). The effect of wind on the distribution of chlorophyll a and crustacean plankton in a shallow eutrophic reservoir. *Journal of Applied Ecology*, *13*(3), 667–690. https://doi.org/10.2307/2402246

George, D. G., & Heaney, S. I. (1978). Factors influencing the spatial distribution of phytoplankton in a small productive lake. *Journal of Ecology*, *66*(1), 133–155. https://doi.org/10.2307/2259185

Goodwin, K., Caraco, N., & Cole, J. (2008). Temporal dynamics of dissolved oxygen in a floating-leaved macrophyte bed. *Freshwater Biology*, *53*(8), 1632–1641. https://doi.org/10.1111/j.1365-2427.2008.01983.x

Grasset, C., Mendonça, R., Villamor Saucedo, G., Bastviken, D., Roland, F., & Sobek, S. (2018). Large but variable methane production in anoxic freshwater sediment upon addition of allochthonous and autochthonous organic matter. *Limnology and Oceanography*, *63*(4), 1488–1501. https://doi.org/10.1002/lno.10786

Harrits, S. M., & Hanson, R. S. (1980). Stratification of aerobic methane-oxidizing organisms in Lake Mendota, Madison, Wisconsin. *Limnology and Oceanography*, *25*(3), 412–421. https://doi.org/10.4319/lo.1980.25.3.0412

Hart, J., Dugan, H., Carey, C., Stanley, E., & Hanson, P. (2017). Lake Mendota carbon and greenhouse gas measurements at North Temperate Lakes LTER 2016. https://doi.org/10.6073/pasta/c50d70814e94266851d13cfdde18b6f6

Heiskanen, J. J., Mammarella, I., Haapanala, S., Pumpanen, J., Vesala, T., Macintyre, S., & Ojala, A. (2014). Effects of cooling and internal wave motions on gas transfer coefficients in a boreal lake. *Tellus B: Chemical and Physical Meteorology*, *66*(1), 22827. https://doi.org/10.3402/tellusb.v66.22827

Hengl, T. (2006). Finding the right pixel size. *Computers and Geosciences*, *32*(9), 1283–1298. https://doi.org/10.1016/j.cageo.2005.11.008

Hofmann, H. (2013). Spatiotemporal distribution patterns of dissolved methane in lakes: How accurate are the current estimations of the diffusive flux path? *Geophysical Research Letters*, *40*, 2779–2784. https://doi.org/10.1002/grl.50453

Hofmann, H., Federwisch, L., & Peeters, F. (2010). Wave-induced release of methane: Littoral zones as source of methane in lakes. *Limnology and Oceanography*, *55*(5), 1990–2000. https://doi.org/10.4319/lo.2010.55.5.1990

Holgerson, M. A., & Raymond, P. A. (2016). Large contribution to inland water CO2 and CH4 emissions from very small ponds. *Nature Geoscience*, *9*(3), 222–226. https://doi.org/10.1038/ngeo2654

Homer, C. G., Dewitz, J. A., Yang, L., Jin, S., Danielson, P., Xian, G., et al. (2015). Completion of the 2011 National Land Cover Database for the conterminous United States—Representing a decade of land cover change information. *Photogrammetric Engineering and Remote Sensing*, *81*(5), 345–354.

Huttunen, J. T., Alm, J., Liikanen, A., Juutinen, S., Larmola, T., Hammar, T., et al. (2003). Fluxes of methane, carbon dioxide and nitrous oxide in boreal lakes and potential anthropogenic effects on the aquatic greenhouse gas emissions. *Chemosphere*, *52*(3), 609–621. https://doi.org/10.1016/S0045-6535(03)00243-1

Jones, J. R., Obrecht, D. V., Graham, J. L., Balmer, M. B., Filstrup, C. T., & Downing, J. A. (2016). Seasonal patterns in carbon dioxide in 15 mid-continent (USA) reservoirs. *Inland Waters*, *6*(2), 265–272. https://doi.org/10.5268/IW-6.2.982

Juutinen, S., Rantakari, M., Kortelainen, P., Huttunen, J. T., Larmola, T., Alm, J., et al. (2009). Methane dynamics in different boreal lake types. *Biogeosciences*, *6*(2), 209–223. https://doi.org/10.5194/bg-6-209-2009

Kankaala, P., Taipale, S., Nykänen, H., & Jones, R. I. (2007). Oxidation, efflux, and isotopic fractionation of methane during autumnal turnover in a polyhumic, boreal lake. *Journal of Geophysical Research*, *112*, G02003. https://doi.org/10.1029/2006JG000336

Karlsson, J., Giesler, R., Persson, J., & Lundin, E. (2013). High emission of carbon dioxide and methane during ice thaw in high latitude lakes. *Geophysical Research Letters*, *40*, 1123–1127. https://doi.org/10.1002/grl.50152

Lathrop, R. C., & Carpenter, S. R. (2013). Water quality implications from three decades of phosphorus loads and trophic dynamics in the Yahara chain of lakes. *Inland Waters*, *4*(1), 1–14. https://doi.org/10.5268/IW-4.1.680

Lauster, G. H., Hanson, P. C., & Kratz, T. K. (2006). Gross primary production and respiration differences among littoral and pelagic habitats in northern Wisconsin lakes. *Canadian Journal of Fisheries and Aquatic Sciences*, *63*(5), 1130–1141. https://doi.org/10.1139/f06-018

Lead P.I NTL., Magnuson, J., Carpenter, S., & Stanley, E. (2010). North Temperate Lakes LTER: Chemical limnology of primary study lakes: Nutrients, pH and carbon 1981–current. https://doi.org/10.6073/pasta/a93c363d2baf94dbd6bb0b34df53648a

Maberly, S. C. (1996). Diel, episodic and seasonal changes in pH and concentrations of inorganic carbon in a productive lake. *Freshwater Biology*, *35*(3), 579–598. https://doi.org/10.1111/j.1365-2427.1996.tb01770.x

Maberly, S. C., Barker, P. A., Stott, A. W., & De Ville, M. M. (2013). Catchment productivity controls CO2 emissions from lakes. *Nature Climate Change*, *3*(4), 391–394. https://doi.org/10.1038/nclimate1748

MacIntyre, S., Wanninkhof, R., & Chanton, J. P. (1995). Trace gas exchange across the air-water interface in freshwater and coastal marine environments. In P. A. Matson, & R. C. Harriss (Eds.), *Biogenic trace gases: measuring emissions from soil and water*, (pp. 52–97). Blackwell.

Mackay, E. B., Jones, I. D., Folkard, A. M., & Thackeray, S. J. (2011). Transition zones in small lakes: The importance of dilution and biological uptake on lake-wide heterogeneity. *Hydrobiologia*, *678*(1), 85–97. https://doi.org/10.1007/s10750-011-0825-y

Mackay, E. B., Jones, I. D., Thackeray, S. J., & Folkard, A. M. (2011). Spatial heterogeneity in a small, temperate lake during archetypal weak forcing conditions. *Fundamental and Applied Limnology*, *179*(1), 27–40. https://doi.org/10.1127/1863-9135/2011/0179-0027

Makarewicz, J. C., Lewis, T. W., Boyer, G. L., & Edwards, W. J. (2012). The influence of streams on nearshore water chemistry, Lake Ontario. *Journal of Great Lakes Research*, *38*, 62–71. https://doi.org/10.1016/j.jglr.2012.02.010

Marchand, P., & Gill, D. (2018). waver: Calculate fetch and wave energy. Retrieved from https://cran.r-project.org/package=waver

McDonald, C. P., Stets, E. G., Striegl, R. G., & Butman, D. (2013). Inorganic carbon loading as a primary driver of dissolved carbon dioxide concentrations in the lakes and reservoirs of the contiguous United States. *Global Biogeochemical Cycles*, *27*, 285–295. https://doi.org/10.1002/gbc.20032

Moss, B. (2011). Allied attack: Climate change and eutrophication. *Inland Waters*, *1*(2), 101–105. https://doi.org/10.5268/IW-1.2.359

Murase, J., Sakai, Y., Kametani, A., & Sugimoto, A. (2005). Dynamics of methane in mesotrophic Lake Biwa, Japan. *Ecological Research*, *20*(3), 377–385. https://doi.org/10.1007/s11284-005-0053-x

Myhre, G., Shindell, D., Bréon, F.-M., Collins, W., Fuglestvedt, J., Huang, J., et al. (2013). Anthropogenic and natural radiative forcing. In T. F. Stocker, D. Qin, G.-K. Plattner, M. Tignor, S. K. Allen, J. Boschung, A. Nauels, Y. Xia, V. Bex, & P. M. Midgley (Eds.), *Climate change 2013: The physical science basis: Working Group I Contribution to the Fifth Assessment Report of the Intergovernmental Panel on Climate Change* (Vol. 9781107057, (pp. 659–740). Cambridge, United Kingdom and New York, NY, USA: Cambridge University Press. https://doi.org/10.1017/CBO9781107415324.018

Natchimuthu, S., Sundgren, I., Gålfalk, M., Klemedtsson, L., & Bastviken, D. (2017). Spatiotemporal variability of lake pCO2 and CO2 fluxes in a hemiboreal catchment. *Journal of Geophysical Research: Biogeosciences*, *122*, 30–49. https://doi.org/10.1002/2016JG003449

Natchimuthu, S., Sundgren, I., Gålfalk, M., Klemedtsson, L., Crill, P., Danielsson, Å., & Bastviken, D. (2016). Spatio-temporal variability of lake CH4 fluxes and its influence on annual whole lake emission estimates. *Limnology and Oceanography*, *61*(S1), S13–S26. https://doi.org/10.1002/lno.10222

Nepf, H. M., & Vivoni, E. R. (2000). Flow structure in depth-limited, vegetated flow. *Journal of Geophysical Research*, *105*(C12), 28,547–28,557. https://doi.org/10.1029/2000JC900145

Ouyang, Z., Shao, C., Chu, H., Becker, R., Bridgeman, T., Stepien, C., et al. (2017). The effect of algal blooms on carbon emissions in western Lake Erie: An integration of remote sensing and eddy covariance measurements. *Remote Sensing*, *9*(1), 44. https://doi.org/10.3390/rs9010044

Paranaíba, J. R., Barros, N., Mendonça, R., Linkhorst, A., Isidorova, A., Roland, F., et al. (2018). Spatially resolved measurements of CO2 and CH4 concentration and gas-exchange velocity highly influence carbon-emission estimates of reservoirs. *Environmental Science & Technology*, *52*(2), 607–615. https://doi.org/10.1021/acs.est.7b05138

Paytan, A., Lecher, A. L., Dimova, N., Sparrow, K. J., Kodovska, F. G.-T., Murray, J., et al. (2015). Methane transport from the active layer to lakes in the Arctic using Toolik Lake, Alaska, as a case study. *Proceedings of the National Academy of Sciences*, *112*(12). https://doi.org/10.1073/pnas.1417392112

Pebesma, E. J. (2004). Multivariable geostatistics in S: The gstat package. *Computers and Geosciences*, *30*(7), 683–691. https://doi.org/10.1016/j.cageo.2004.03.012

Peeters, F., Atamanchuk, D., Tengberg, A., Encinas-Fernández, J., & Hofmann, H. (2016). Lake metabolism: Comparison of lake metabolic rates estimated from a diel CO2 and the common diel O2 technique. *PLoS ONE*, *11*(12). https://doi.org/10.1371/journal.pone.0168393

Peeters, F., Fernandez, J. E., & Hofmann, H. (2019). Sediment fluxes rather than oxic methanogenesis explain diffusive CH4 emissions emissions from lakes and reservoirs. *Scientific Reports*, *9*(1), 243. https://doi.org/10.1038/s41598-018-36530-w

Peixoto, R. B., Marotta, H., Bastviken, D., & Enrich-Prast, A. (2016). Floating aquatic macrophytes can substantially offset open water CO2 emissions from tropical floodplain lake ecosystems. *Ecosystems*, *19*(4), 724–736. https://doi.org/10.1007/s10021-016-9964-3

Pinel-Alloul, P. (1995). Spatial heterogeneity as a multiscale characteristic of zooplankton community. *Hydrobiologia*, *300*(1), 17–42. https://doi.org/10.1007/BF00024445

Plummer, L. N., & Busenberg, E. (1982). The solubilities of calcite, aragonite and vaterite in CO2-H2O solutions between 0 and 90°C, and an evaluation of the aqueous model for the system CaCO3-CO2-H2O. *Geochimica et Cosmochimica Acta*, *46*(6), 1011–1040. https://doi.org/10.1016/0016-7037(82)90056-4

Podgrajsek, E., Sahlee, E., & Rutgersson, A. (2015). Diel cycle of lake-air CO2 flux from a shallow lake and the impact of waterside convection on the transfer velocity. *Journal of Geophysical Research: Biogeosciences*, *120*, 29–38. https://doi.org/10.1002/2014JG002781

R Core Team. (2018). R: A language and environment for statistical computing. Vienna, Austria: R Foundation for Statistical Computing.

Rasilo, T., Prairie, Y. T., & del Giorgio, P. A. (2015). Large-scale patterns in summer diffusive CH4 fluxes across boreal lakes, and contribution to diffusive C emissions. *Global Change Biology*, *21*(3), 1124–1139. https://doi.org/10.1111/gcb.12741

Raymond, P. A., Hartmann, J., Lauerwald, R., Sobek, S., McDonald, C., Hoover, M., et al. (2013). Global carbon dioxide emissions from inland waters. *Nature*, *503*(7476), 355–359. https://doi.org/10.1038/nature12760

Raymond, P. A., Zappa, C. J., Butman, D., Bott, T. L., Potter, J., Mulholland, P., et al. (2012). Scaling the gas transfer velocity and hydraulic geometry in streams and small rivers. *Limnology and Oceanography: Fluids and Environments*, *2*(1), 41–53. https://doi.org/10.1215/21573689-1597669

Read, J. S., Hamilton, D. P., Desai, A. R., Rose, K. C., MacIntyre, S., Lenters, J. D., et al. (2012). Lake-size dependency of wind shear and convection as controls on gas exchange. *Geophysical Research Letters*, *39*, L09405. https://doi.org/10.1029/2012GL051886

Reed, D. E., Dugan, H. A., Flannery, A. L., & Desai, A. R. (2018). Carbon sink and source dynamics of a eutrophic deep lake using multiple flux observations over multiple years. *Limnology and Oceanography Letters*, *3*(3), 285–292. https://doi.org/10.1002/lol2.10075

Rinke, K., Huber, A. M. R., Kempke, S., Eder, M., Wolf, T., Probst, W. N., & Rothhaupt, K. O. (2009). Lake-wide distributions of temperature, phytoplankton, zooplankton, and fish in the pelagic zone of a large lake. *Limnology and Oceanography*, *54*(4), 1306–1322. https://doi.org/10.4319/lo.2009.54.4.1306

Rudd, J. W. M., & Hamilton, R. D. (1978). Methane cycling in Lake 227 and its effects on whole lake metabolism. *Limnology and Oceanography*, *23*(2), 337–348. https://doi.org/10.4319/lo.1978.23.2.0337

Salmi, P., & Salonen, K. (2016). Regular build-up of the spring phytoplankton maximum before ice-break in a boreal lake. *Limnology and Oceanography*, *61*(1), 240–253. https://doi.org/10.1002/lno.10214

Schilder, J., Bastviken, D., Van Hardenbroek, M., Kankaala, P., Rinta, P., Stötter, T., & Heiri, O. (2013). Spatial heterogeneity and lake morphology affect diffusive greenhouse gas emission estimates of lakes. *Geophysical Research Letters*, *40*, 5752–5756. https://doi.org/10.1002/2013GL057669

Sobek, S., Tranvik, L. J., & Cole, J. J. (2005). Temperature independence of carbon dioxide supersaturation in global lakes. *Global Biogeochemical Cycles*, *19*, GB2003. https://doi.org/10.1029/2004GB002264

Sommer, U., Adrian, R., de Senerpont Domis, L., Elser, J. J., Gaedke, U., Ibelings, B., et al. (2012). Beyond the plankton ecology group (PEG) model: Mechanisms driving plankton succession. *Annual Review of Ecology, Evolution, and Systematics*, *43*(1), 429–448. https://doi.org/10.1146/annurev-ecolsys-110411-160251

Sommer, U., Gliwicz, Z. M., Lampert, W. I., & Duncan, A. (1986). The PEG-model of seasonal succession of planktonic events in fresh waters. *Archiv Fur Hydrobiologie*, *44*(3), 393–431. https://doi.org/10.1111/j.1469-185X.1969.tb01218.x

Stanley, E. H., Casson, N. J., Christel, S. T., Crawford, J. T., Loken, L. C., & Oliver, S. K. (2016). The ecology of methane in streams and rivers: Patterns, controls, and global significance. *Ecological Monographs*, *86*(2), 146–171. https://doi.org/10.1890/15-1027

Stets, E. G., Butman, D., Mcdonald, C. P., Stackpoole, S. M., DeGrandpre, M. D., & Striegl, R. G. (2017). Carbonate buffering and metabolic controls on carbon dioxide in rivers. *Global Biogeochemical Cycles*, *31*, 663–677. https://doi.org/10.1002/2016GB005578

Striegl, R. G., Kortelainen, P., Chanton, J. P., Wickland, K. P., Bugna, G. C., & Rantakari, M. (2001). Carbon dioxide partial pressure and 13C content of north temperate and boreal lakes at spring ice melt. *Limnology and Oceanography*, *46*(4), 941–945. https://doi.org/10.4319/lo.2001.46.4.0941

Tang, K. W., McGinnis, D. F., Ionescu, D., & Grossart, H.-P. (2016). Methane production in oxic lake waters potentially increases aquatic methane flux to air. *Environmental Science & Technology Letters*, *3*(6), 227–233. https://doi.org/10.1021/acs.estlett.6b00150

Tranvik, L. J., Downing, J. A., Cotner, J. B., Loiselle, S. A., Striegl, R. G., Ballatore, T. J., et al. (2009). Lakes and reservoirs as regulators of carbon cycling and climate. *Limnology and Oceanography*, *54*(6part2), 2298–2314. https://doi.org/10.4319/lo.2009.54.6_part_2.2298

Turner, M. G., & Chapin, F. S. (2005). Causes and consequences of spatial heterogeneity in ecosystem function. In G. M. Lovett, M. G. Turner, C. G. Jones, & K. C. Weathers (Eds.), *Ecosystem Function in Heterogeneous Landscapes*, (pp. 9–30). New York, NY, NY: Springer New York. https://doi.org/10.1007/0-387-24091-8_2

Vachon, D., & Prairie, Y. T. (2013). The ecosystem size and shape dependence of gas transfer velocity versus wind speed relationships in lakes. *Canadian Journal of Fisheries and Aquatic Sciences*, *70*(12), 1757–1764. https://doi.org/10.1139/cfjas-2013-0241

Van de Bogert, M. C., Bade, D. L., Carpenter, S. R., Cole, J. J., Pace, M. L., Hanson, P. C., & Langman, O. C. (2012). Spatial heterogeneity strongly affects estimates of ecosystem metabolism in two north temperate lakes. *Limnology and Oceanography*, *57*(6), 1689–1700. https://doi.org/10.4319/lo.2012.57.6.1689

Webb, J. R., Maher, D. T., & Santos, I. R. (2016). Automated, in situ measurements of dissolved CO2, CH4, and δ13C values using cavity enhanced laser absorption spectrometry: Comparing response times of air-water equilibrators. *Limnology and Oceanography: Methods*, *14*(5), 323–337. https://doi.org/10.1002/lom3.10092

West, W. E., Coloso, J. J., & Jones, S. E. (2012). Effects of algal and terrestrial carbon on methane production rates and methanogen community structure in a temperate lake sediment. *Freshwater Biology*, *57*(5), 949–955. https://doi.org/10.1111/j.1365-2427.2012.02755.x

West, W. E., Creamer, K. P., & Jones, S. E. (2016). Productivity and depth regulate lake contributions to atmospheric methane. *Limnology and Oceanography*, *61*(S1), S51–S61. https://doi.org/10.1002/lno.10247

Wik, M., Thornton, B. F., Bastviken, D., Uhlbäck, J., & Crill, P. M. (2016). Biased sampling of methane release from northern lakes: A problem for extrapolation. *Geophysical Research Letters*, *43*, 1256–1262. https://doi.org/10.1002/2015GL066501

Wilhelm, E., Battino, R., & Wilcock, R. J. (1977). Low-pressure solubility of gases in liquid water. *Chemical Reviews*, *77*(2), 219–262. https://doi.org/10.1021/cr60306a003

Winfrey, M. R., & Zeikus, J. G. (1979). Anaerobic metabolism of immediate methane precursors in Lake Mendota. *Applied and Environmental Microbiology*, *37*(2), 244–253.

Winslow, L. A., Zwart, J. A., Batt, R. D., Dugan, H. A., Woolway, R. I., Corman, J. R., et al. (2016). LakeMetabolizer: An R package for estimating lake metabolism from free-water oxygen using diverse statistical models. *Inland Waters*, *6*(4), 622–636. https://doi.org/10.5268/IW-6.4.883

Wynne, T. T., & Stumpf, R. P. (2015). Spatial and temporal patterns in the seasonal distribution of toxic cyanobacteria in western Lake Erie from 2002–2014. *Toxins*, *7*(5), 1649–1663. https://doi.org/10.3390/toxins7051649

Yvon-Durocher, G., Allen, A. P., Bastviken, D., Conrad, R., Gudasz, C., St-Pierre, A., et al. (2014). Methane fluxes show consistent temperature dependence across microbial to ecosystem scales. *Nature*, *507*(7493), 488–491. https://doi.org/10.1038/nature13164

Zeikus, J. G., & Winfrey, M. R. (1976). Temperature limitation of methanogenesis in aquatic sediments. *Applied and Environmental Microbiology*, *31*(1), 99–107.

Zhang, Y., Shi, K., Zhou, Y., Liu, X., & Qin, B. (2016). Monitoring the river plume induced by heavy rainfall events in large, shallow, Lake Taihu using MODIS 250m imagery. *Remote Sensing of Environment*, *173*, 109–121. https://doi.org/10.1016/j.rse.2015.11.020